

# EVIDENCE FOR EARLY FILAMENTARY ACCRETION FROM THE ANDROMEDA GALAXY'S THIN PLANE OF SATELLITES

TOBIAS BUCK<sup>1</sup>, ANDREA V. MACCIÒ<sup>2</sup> AND AARON A. DUTTON<sup>3</sup>  
 Max-Planck Institut für Astronomie, Königstuhl 17, D-69117 Heidelberg, Germany  
*accepted for publication in ApJ Letters*

## Abstract

Recently it has been shown that a large fraction of the dwarf satellite galaxies orbiting the Andromeda galaxy are surprisingly aligned in a thin, extended and kinematically coherent planar structure. The presence of such a structure seems to challenge the current Cold Dark Matter paradigm of structure formation, which predicts a more uniform distribution of satellites around central objects. We show that it is possible to obtain a thin, extended, rotating plane of satellites resembling the one in Andromeda in cosmological collisionless simulations based on the Cold Dark Matter model. Our new high resolution simulations show a correlation between the formation time of the dark matter halo and the thickness of the plane of satellites. Our simulations have a high incidence of satellite planes as thin, extended, and as rich as the one in Andromeda and with a very coherent kinematic structure when we select high concentration/early forming halos. By tracking the formation of the satellites in the plane we show that they have been mainly accreted onto the main object along thin dark matter filaments at high redshift. Our results show that the presence of a thin, extended, rotating plane of satellites is not a challenge for the Cold Dark Matter paradigm, but actually supports one of the predictions of this paradigm related to the presence of filaments of dark matter around galaxies at high redshift.

*Subject headings:* galaxies: individual Andromeda — galaxies: dwarf — galaxies: kinematics and dynamics — galaxies: formation — dark matter — methods: numerical

## 1. INTRODUCTION

The success of the currently favored model of structure formation, the Cold Dark Matter model, lies in its outstanding accordance with observations on large scales (Tegmark et al. 2004; Springel et al. 2005). However, over the last years several problems on galactic and sub galactic scales have been reported, e.g. the missing satellite (Klypin et al. 1999; Moore et al. 1999) and cusp-core (Moore 1994; Boylan-Kolchin et al. 2011) problems. A potential solution to these issues lies in an inappropriate comparison between observations and simulations which consider only the dark matter component. Cosmological simulations including baryonic physics (gas and stars) have been shown to be able to ease those problems and to bring the CDM model in agreement with observations (Benson et al. 2007; Macciò et al. 2010; Governato et al. 2010; Di Cintio et al. 2014; Brooks & Zolotov 2014).

Recent observations of dwarf satellite galaxies around Andromeda (McConnachie & Irwin 2006; Koch & Grebel 2006; Ibata et al. 2013), and possibly also around the Milky Way (Metz et al. 2008), have suggested these satellites to align in a rotationally supported disc. Ibata et al. (2013) find that 15 out of 27 satellites in the Pan-Andromeda Archaeological Survey (PAndAS, McConnachie et al. 2009) lie in a thin plane of thickness  $(12.6 \pm 0.6)$  kpc. Furthermore, using line-of-sight velocities, they report 13 of the satellites in the plane to corotate. This kind of spatial and kinematic alignment is not easily found in Cold Dark Matter simulations (Pawlowski et al. 2014; Pawlowski & McGaugh 2014; Ibata et al.

2014a), though not impossible (Libeskind et al. 2009; Ibata et al. 2014a). Furthermore there are other studies which have searched for planes of satellites in hydrodynamical simulations (Lovell et al. 2011; Gillet et al. 2015, and references therein). There have been indications that filamentary accretion of subhalos can lead to anisotropic spatial distributions of them (Libeskind et al. 2009; Lovell et al. 2011; Libeskind et al. 2014). Nevertheless none of the previous studies was able to closely reproduce the parameters of Andromeda's plane of satellites (number of members, thickness, corotation, and extension). Since the accretion and distribution of dwarf galaxies is primarily governed by the global gravitational potential, which is dominated by the dark matter distribution, this issue has raised (again) the question whether the Cold Dark Matter model is correct or, conversely, needs to be revised.

In this letter we present new high resolution “zoom-in” dark matter only simulations of Andromeda sized dark matter halos which reveal thin rotating planes of sub halos like in the case of Andromeda. The key insight that enables us to solve this puzzle is that halos formed through filamentary accretion should form earlier and thus can be selected by their higher than average present day dark halo concentrations.

This paper is organized as follows: In §2 we present the simulations, including the host halo selection criteria and our plane finding algorithm. In section §3 we then present the results of our study and in §4 we present our conclusions.

## 2. SIMULATIONS

We performed 21 high resolution “zoom-in” dark matter only simulations using the N-body code PKDGRAV2

<sup>1</sup> buck@mpia.de  
<sup>2</sup> maccio@mpia.de  
<sup>3</sup> dutton@mpia.de

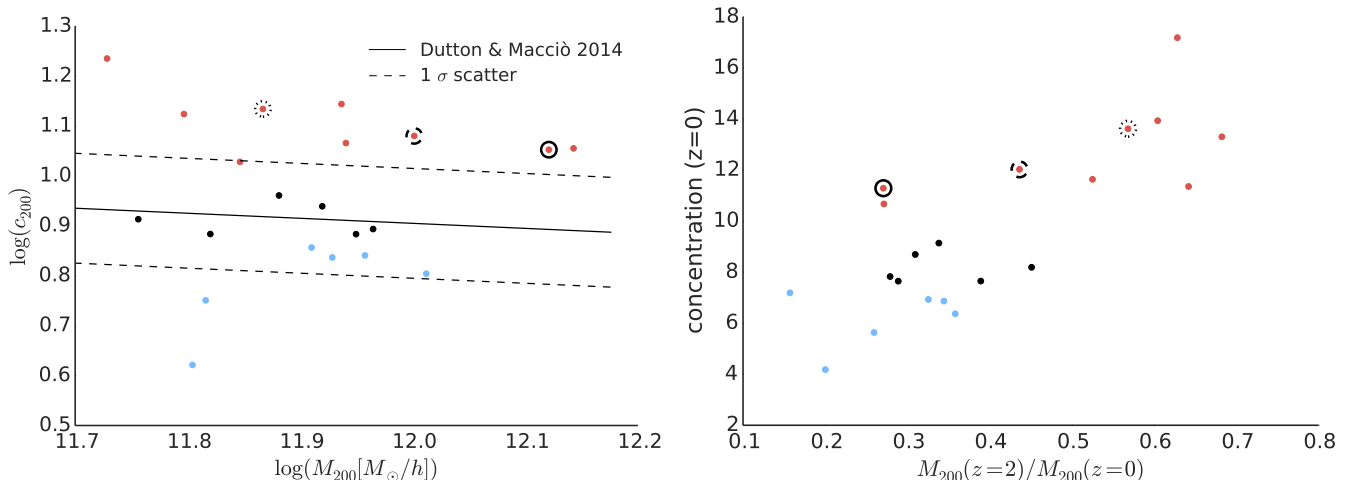


FIG. 1.— *Left panel*: Concentration mass relation. This diagram shows the concentration as a function of mass of the high resolution halos. The solid line is the average relation from Dutton & Macciò (2014). The dashed line indicates the  $1\sigma$  scatter of this relation. Color coding shows the division of the halos into high, average and low concentration. *Right panel*: Mass growth vs. concentration. The plot shows the concentration at  $z = 0$  as a function of mass at  $z = 2$  in terms of the present day mass. Strongly growing halos (late forming) are located on the left while least growing halos (early forming) are located on the right. The color coding shows the division of the halos into high, average and low concentration. The halos with satellite planes coming closest to the values of Andromeda are marked by black circles. The solid one is *halo A*, the dashed one is *halo B*.

(Stadel 2001, 2013). We select Andromeda-like mass halos ( $5 \times 10^{11} < M_{200}/[h^{-1}M_{\odot}] < 1.5 \times 10^{12}$ ), where the halo mass is defined with respect to 200 times the critical density of the universe. The halos were selected from three cosmological boxes of sides 30, 60 and  $80 h^{-1}\text{Mpc}$  from Dutton & Macciò (2014) which used cosmological parameters from the Planck Collaboration (2014):  $\Omega_m = 0.3175$ ,  $h = 0.671$ ,  $\sigma_8 = 0.8344$ ,  $n = 0.9624$ .

Initial conditions for zoom-in simulations were created using a modified version of the *grafic2* package (Bertschinger 2001) as described in (Penzo et al. 2014). The refinement level was chosen to maintain a roughly constant relative resolution, e.g.  $\sim 10^7$  dark matter particles per halo with particle masses of  $\sim 10^5 h^{-1}M_{\odot}$ . This allows us to reliably resolve substructure down to  $\sim 5 \times 10^7 h^{-1}M_{\odot}$ . The force softening of our simulations ranges between  $0.25 h^{-1} \text{ kpc}$  and  $0.36 h^{-1} \text{ kpc}$ .

### 2.1. Halo concentration and formation time

Aside from halo mass, the only other selection criteria for our objects is the concentration, which is a proxy for halo formation time (Wechsler et al. 2002). The right panel of Fig. 1 shows the concentration at  $z = 0$  as a function of the mass growth since  $z = 2$ . The clear correlation validates our approach of using the concentration as a first proxy for the halo formation time.

The reasoning behind such a choice is that, at a **fixed mass** at the present time, early forming halos are more likely to form at the nodes of intersection of a few filaments of the cosmic web, while typical halos tend to reside inside such filaments (Dekel et al. 2009). One then might expect that, rare, early forming halos would accrete satellites from a few streams that are narrow compared to the halo size, while typical halos accrete satellites from a wide angle in a practically spherical pattern.

In the left panel of Fig. 1 we show the concentration-mass relation of our high resolution halos. Here the concentration is defined as  $c_{200} = R_{200}/r_{-2}$ , where  $R_{200}$  is the virial radius, and  $r_{-2}$  is the radius where the logarithmic slope of the density profile is  $-2$ . We select roughly

equal number of high (red points), average (black points) and low (blue points) concentration halos (see Fig. 1).

The solid line is the power law fit from Dutton & Macciò (2014), while the dashed ones show the  $1\sigma$  intrinsic scatter of 0.11 dex around the mean. Our high concentration halos have on average an offset of about  $2\sigma$  from the mean relation. This means these halos are the rarest 2.3% of the whole population. In a random sample of halos it would thus require  $\sim 40$  simulations to recover such rare halo. This helps to explain why previous high resolution simulations were unable to reproduce the observed properties of the satellite distribution around the Andromeda galaxy: they simply did not sample enough halos to find the rarer earliest forming ones.

### 2.2. Satellite selection

Our simulations reveal hundreds of resolved subhalos which have to be matched to actual luminous galaxies. Galaxy formation models robustly predict the luminous subhalos to be the ones most massive at infall times (Kravtsov et al. 2004; Conroy et al. 2006; Vale & Ostriker 2006). Thus, we select a sample of the 30 most massive sub halos at the time of the accretion, where we restrict our analysis to sub halos within the virial radius of the host halo ( $\sim 200 \text{ kpc}$ ).

Although observations around Andromeda use a special selection function given by the peculiarities of the Pan-Andromeda Archaeological Survey (PAndAS) (McConnachie et al. 2009), we choose not to reproduce the selection function for a number of reasons. Firstly, it requires surface-brightness information which we do not have in our (dark matter only) simulations. Secondly, the PAndAS footprint is unique to the Andromeda galaxy, being non-circular, and including a region around its most massive satellite M33. Thus it would not make sense to apply the same footprint to a cosmological simulation. Thirdly, the spatial depth of the survey is somewhat uncertain due to the difficulty of measuring accurate distances to the satellites. Rather, we apply a simple, reproduceable, and physically motivated selec-

tion criteria. As our satellite population we select the most massive sub halos (at the time of infall) within the  $z = 0$  virial radius,  $R_{\text{vir}}$ . Choosing satellites within the virial radius leaves us with a bigger volume ( $\approx R_{\text{vir}}^3$ ) compared to the observations and hence we use a number of 30 satellites instead of 27. Furthermore, there is some arbitrariness in the number of satellites related to Andromeda. Nine known satellites (two that lie inside the PAndAS field, and seven that lie outside) were not considered by Ibata et al. (2014b); Conn et al. (2013). Nevertheless we experimented with sample sizes of 25, 27 and 30 satellites and found no major differences in the plane statistics.

### 2.3. Plane finding algorithm

In order to find planes in the distribution of sub halos we generate a random sample of planes defined by their normal vector. All planes include the center of the main halo. To uniformly cover the whole volume we generate 100,000 random planes with a fixed thickness of  $2\Delta = 40h^{-1}$  kpc. After specifying a plane we calculate the distance of every satellite to this plane. A satellite is considered to lie in the plane if its distance to the plane is smaller than  $\Delta$ . For each plane we calculate the number of satellites in the plane and its root-mean-square thickness  $\Delta_{\text{rms}}$ . We then select for every number of satellites in the plane the one which is thinnest and richest to analyze for kinematics (for further details see also Gillet et al. 2015; Ibata et al. 2014b; Conn et al. 2013).

The plane of satellites around Andromeda can be characterized by 4 parameters including the number of satellites in the plane ( $N_{\text{in}}$ ), the number of corotating satellites ( $N_{\text{corot}}$ ), the thickness of the plane ( $\Delta_{\text{rms}}$ ) and its extension. For Andromeda these values are  $N_{\text{in}} = 15$ ,  $N_{\text{corot}} = 13$ ,  $\Delta_{\text{rms}} = 12.6 \pm 0.6$  kpc, and a projected diameter of  $\sim 280$  kpc.

## 3. RESULTS

### 3.1. Plane thickness vs halo concentration

In a first step of our analysis we investigated the correlation between concentration (as a proxy of halo formation time) and thickness of the plane. Fig. 2 shows the plane thickness as a function of the number of satellites in the plane, with lines color coded according to halo concentration. There is a clear dependence of plane thickness on the concentration of the halo. The thinnest planes are only found in the highest concentration (red lines), and hence earliest forming halos. Furthermore, only high concentration halos have planes as thin as observed in Andromeda (assuming 15 members). The smooth relation between plane thickness and number of satellites in the plane suggests that there is an arbitrariness in the number of satellites chosen to be in the plane. We do not see clear evidence of two distinct spatial structures such as a planar and spherical distribution of satellites. We further note that an investigation of the satellite distribution does not reveal a more concentrated satellite distribution in high concentration halos, which might trivially explain the dependence of plane thickness on concentration that we find.

### 3.2. Corotation vs number of satellites in plane

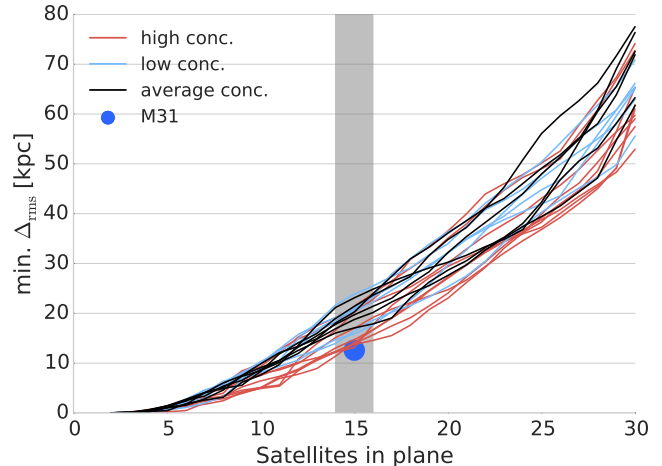


FIG. 2.— Minimal root-mean-square thickness,  $\min. \Delta_{\text{rms}}$ , of planes as a function of number of satellites in the plane. Each line represents a different dark matter halo. Red lines show high concentration halos, blue lines show low concentration halos and black lines show average concentration halos. The thinnest planes occur in the highest concentration halos. The blue dot shows the rms value of the plane of satellites observed around Andromeda (Ibata et al. (2013); Conn et al. (2013)). The grey area represents a nominal uncertainty in the number of satellites in the plane around Andromeda of  $\pm 1$ .

Fig. 3 shows the outcome of our plane finding algorithm for the two (early forming) halos best matching the values of Andromeda (halo A:  $N_{\text{in}} = 15$ ,  $N_{\text{corot}} = 14$ ,  $\Delta_{\text{rms}} = 15.8$  kpc, diameter  $\sim 220$  kpc; and halo B:  $N_{\text{in}} = 15$ ,  $N_{\text{corot}} = 13$ ,  $\Delta_{\text{rms}} = 12.9$  kpc,  $\sim 450$  kpc). The plots show for every value of the number of satellites in the plane,  $N_{\text{in}}$ , the number of corotating satellites,  $N_{\text{corot}}$ . Every dot in the plot represents a different plane. In both halos one can find planes with up to 12 members that have a 100% corotation fraction. One can always find planes with no coherent kinematics (i.e., a corotation fraction of 50%). The points are color coded according to the thickness of the plane  $\Delta_{\text{rms}}$ . As would be expected, planes with more satellites tend to be thicker. The thickness of the plane is also to first order independent of the corotation fraction, except at the highest corotation fractions.

This figure also shows that there is some arbitrariness in choosing the *best* plane from a simulation. For example for halo A (left panel in Fig. 3, and upper panel of Fig. 4), we can find a plane with 15 satellites and 14 corotating (one more than Andromeda). If we restrict to a plane of 14 satellites (instead of 15) we still find a large corotation fraction ( $N_{\text{corot}} = 13$ ) but in a thinner plane  $\Delta_{\text{rms}} = 13.9$  kpc, which is consistent with the Andromeda value.

We are also able to find a thin plane even richer in number of satellites and coherent motion as the one found around Andromeda. For example, in *halo A* we are able to find planes consisting of up to 17 satellites from which 13 share the same rotation direction (see left panel in Fig. 3).

### 3.3. Visual impression of planes matching Andromeda

Fig. 4 shows one particular projection of two early forming halos with plane parameters coming closest to the ones observed around Andromeda. The left hand side shows the spatial extension and the kinematics of the system, clearly revealing a thin but radially extended

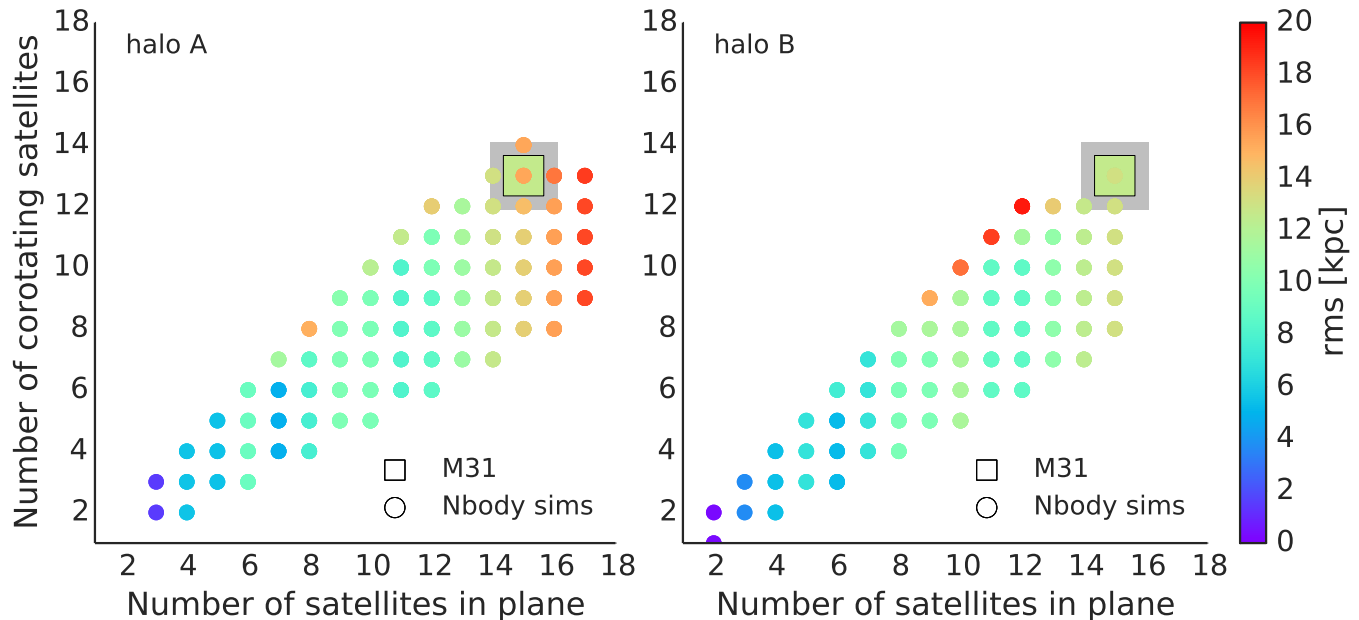


FIG. 3.— Number of corotating satellites vs. number of satellites in the plane for the two best matching high concentration halos (*halo A* (left) & *halo B* (right)). The points are color coded by the rms thickness ( $\Delta_{\text{rms}}$ ) of each plane. The *square* marks the values observed for Andromeda (15 in plane, 13 corotating), where the *grey* shaded area marks the uncertainty of  $\pm 1$  satellite in the plane and  $\pm 1$  corotating satellite. The *dots* show the values of the planes found for this halo.

plane with coherent motion of the satellites around their host. The right hand side shows a dark matter density map of the host halos, with superimposed the two satellite populations, one in the plane (green circles) and one outside the plane (black circles). Such distinct planes were reported before in CDM simulations (Gillet et al. 2015; Ibata et al. 2014a; Pawlowski et al. 2014) but never as rich as the ones found here.

It is worth noticing that previous simulation studies either were limited by the capability of resolving enough (sub)structures, e.g., the Millennium II simulation (Boylan-Kolchin et al. 2009) or, conversely, were limited by very low number statistics of host halos (Gillet et al. 2015), moreover the halos were not selected according to formation time. Since we are able to find planes as rich as the one around Andromeda in at least 3 out of our 20 simulations, the **rarity** of the planes can be explained by the rareness of early forming halos.

### 3.4. Formation scenario

We now move to the question where does this spatial and kinematic coherence come from. By tracing the satellites in the plane back to a redshift of  $z = 3$  we reveal the accretion of the satellites are along dark matter filaments. This can be seen in Fig. 5 where we show a density plot of the main halo and its substructure at redshift  $z = 3$  indicating the satellites in the plane by green circles and the satellites outside the plane by white circles. Providing two different projections these plots prove the connection between accretion along filaments and the property of being in a kinematically coherent plane at redshift  $z = 0$ .

The presence of a plane of satellites in Andromeda seems then to suggest an (unusual) early formation epoch for this galaxy. Such a scenario is consistent with other observational evidences. For its stellar mass ( $\sim 10^{11} M_{\odot}$ )

Andromeda lives in a lower mass dark matter halo than typical galaxies of the same mass (Moster et al. 2010). At these stellar masses the majority of galaxies are bulge-dominated and non star forming, while Andromeda is disk-dominated and star forming, consistent with an early mass accretion history, devoid of recent major mergers. A similar line of reasoning also suggests an early formation epoch for the Milky Way.

## 4. CONCLUSION

We have explored the connection between the formation time of a host dark matter halo and the alignment and coherent kinematics of its subhalos using 21 high-resolution (10 million particles) cosmological N-body simulations. Our key new result is that high concentration (earlier forming) halos tend to have thinner and richer planes. Our simulations show that the presence of a thin, rotating, and extended plane of satellites like the one observed around the Andromeda galaxy is not a challenge for the Cold Dark Matter paradigm. Conversely it supports one of the key predictions of such a model, namely the presence of large filaments of dark matter around galaxies at high redshift and the web-like nature of cosmic structures in the Universe.

The connection we report in this letter between the formation time with the satellite distribution at the present time, opens a new possibility of constraining the topology of the dark matter accretion pattern.

## ACKNOWLEDGMENTS

The authors acknowledge support from the Sonderforschungsbereich SFB 881 The Milky Way System (sub-project A2) of the German Research Foundation (DFG). Simulations have been performed on the THEO clusters of the Max-Planck-Institut fuer Astronomie at the

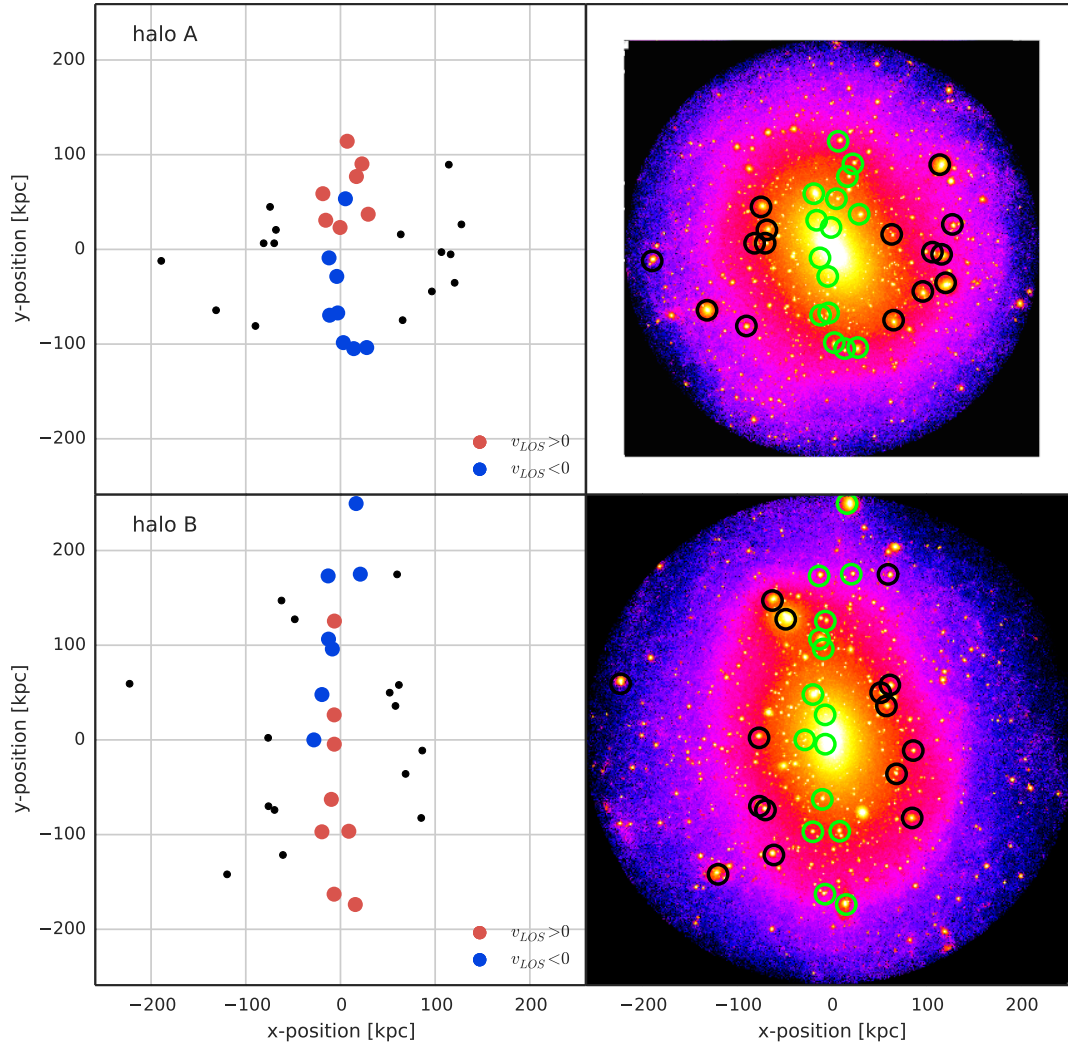


FIG. 4.— Edge on view of planes. The *left* panels show the sign of the line-of-sight velocity of the best matching plane consisting of 15 satellites (colored dots). Black dots show the satellites not in the plane. The *right* panels show high resolution density plots of the halo hosting the best matching plane. *Green circles* indicate the sub halos in the plane and *black circles* indicate sub halos not in the plane. The *upper panels* show *halo A*, while the *lower panels* show *halo B* a slightly more massive halo, also revealing the dependence of radial extension on mass.

Rechenzentrum in Garching. We thank R. van den Bosch

and F. Walter for their comments on an early version of this draft.

#### REFERENCES

- Benson, A. J., Džanović, D., Frenk, C. S., & Sharples, R. 2007, *MNRAS*, 379, 841
- Bertschinger, E. 2001, *ApJS*, 137, 1
- Boylan-Kolchin, M., Bullock, J. S., & Kaplinghat, M. 2011, *MNRAS*, 415, L40
- Boylan-Kolchin, M., Springel, V., White, S. D. M., Jenkins, A., & Lemson, G. 2009, *MNRAS*, 398, 1150
- Brooks, A. M., & Zolotov, A. 2014, *ApJ*, 786, 87
- Conn, A. R., Lewis, G. F., Ibata, R. A., et al. 2013, *ApJ*, 766, 120
- Conroy, C., Wechsler, R. H., & Kravtsov, A. V. 2006, *ApJ*, 647, 201
- Dekel, A., Birnboim, Y., Engel, G., et al. 2009, *Nature*, 457, 451
- Di Cintio, A., Brook, C. B., Macciò, A. V., et al. 2014, *MNRAS*, 437, 415
- Dutton, A. A., & Macciò, A. V. 2014, *MNRAS*, 441, 3359
- Gillet, N., Ocvirk, P., Aubert, D., et al. 2015, *ApJ*, 800, 34
- Governato, F., Brook, C., Mayer, L., et al. 2010, *Nature*, 463, 203
- Ibata, R. A., Ibata, N. G., Lewis, G. F., et al. 2014a, *ApJ*, 784, L6
- . 2014b, *ApJ*, 784, L6
- Ibata, R. A., Lewis, G. F., Conn, A. R., et al. 2013, *Nature*, 493, 62
- Klypin, A., Kravtsov, A. V., Valenzuela, O., & Prada, F. 1999, *ApJ*, 522, 82
- Koch, A., & Grebel, E. K. 2006, *AJ*, 131, 1405
- Kravtsov, A. V., Gnedin, O. Y., & Klypin, A. A. 2004, *ApJ*, 609, 482
- Libeskind, N. I., Frenk, C. S., Cole, S., Jenkins, A., & Helly, J. C. 2009, *MNRAS*, 399, 550
- Libeskind, N. I., Knebe, A., Hoffman, Y., & Gottlöber, S. 2014, *MNRAS*, 443, 1274
- Lovell, M. R., Eke, V. R., Frenk, C. S., & Jenkins, A. 2011, *MNRAS*, 413, 3013
- Macciò, A. V., Kang, X., Fontanot, F., et al. 2010, *MNRAS*, 402, 1995
- McConnachie, A. W., & Irwin, M. J. 2006, *MNRAS*, 365, 902
- McConnachie, A. W., Irwin, M. J., Ibata, R. A., et al. 2009, *Nature*, 461, 66
- Metz, M., Kroupa, P., & Libeskind, N. I. 2008, *ApJ*, 680, 287
- Moore, B. 1994, *Nature*, 370, 629



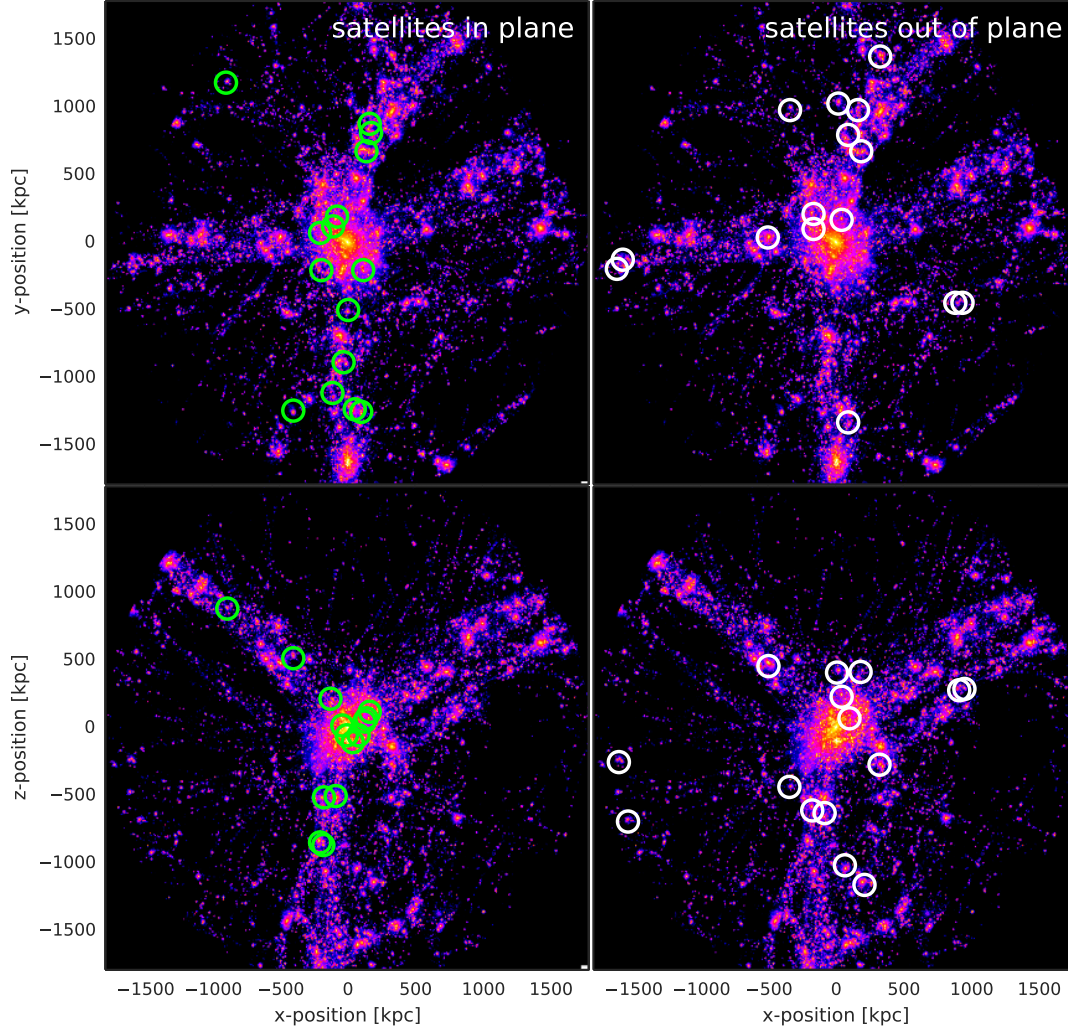


FIG. 5.— High redshift ( $z = 3$ ) density plots of satellite distribution ending up in the plane and outside of the plane of *halo A*. The *left panel* shows density plots of  $x-y$  and  $x-z$ -projections of the satellites ending up in the plane at  $z = 0$  while the *right panel* shows density plots of the  $x-y$  and  $x-z$ -projections of the satellites ending up outside of the plane. The upper panel shows that satellites ending up in the plane are accreted along two filaments coming from opposite sides of the main halo, which set a preferred infall direction. While satellites not ending up in the plane are accreted from everywhere. Comparison with the lower panel shows clearly that satellites ending up in the plane lie within the filaments such that their projection collimates in the center of the halo while halos not ending up in the plane scatter around the main halo indicating that they are not part of the filaments.

Moore, B., Ghigna, S., Governato, F., et al. 1999, *ApJ*, 524, L19  
 Moster, B. P., Somerville, R. S., Maulbetsch, C., et al. 2010, *ApJ*, 710, 903  
 Pawlowski, M. S., & McGaugh, S. S. 2014, *ApJ*, 789, L24  
 Pawlowski, M. S., Famaey, B., Jerjen, H., et al. 2014, *MNRAS*, 442, 2362  
 Penzo, C., Macciò, A. V., Casarini, L., Stinson, G. S., & Wadsley, J. 2014, *MNRAS*, 442, 176  
 Planck Collaboration, Ade, P. A. R., Aghanim, N., et al. 2014, *A&A*, 571, A16  
 Springel, V., White, S. D. M., Jenkins, A., et al. 2005, *Nature*, 435, 629

Stadel, J. 2013, PkdGRAV2: Parallel fast-multipole cosmological code, Astrophysics Source Code Library, ascl:1305.005  
 Stadel, J. G. 2001, PhD thesis, UNIVERSITY OF WASHINGTON  
 Tegmark, M., Strauss, M. A., Blanton, M. R., et al. 2004, *Phys. Rev. D*, 69, 103501  
 Vale, A., & Ostriker, J. P. 2006, *MNRAS*, 371, 1173  
 Wechsler, R. H., Bullock, J. S., Primack, J. R., Kravtsov, A. V., & Dekel, A. 2002, *ApJ*, 568, 52